

Field-theoretic analysis of directed percolation: Three-loop approximationLoran Ts. Adzhemyan,^{1,2} Michal Hnatic^{Ⓧ,2,3,4,*}, Ella V. Ivanova^{Ⓧ,5}, Mikhail V. Kompaniets,^{1,2,†}
Tomáš Lučivjanský^{Ⓧ,4,‡} and Lukáš Mižišin^{Ⓧ,2,§}¹*Sankt Petersburg State University, St. Petersburg 199034, Russian Federation*²*Bogolyubov Laboratory of Theoretical Physics, Joint Institute for Nuclear Research, 141980 Dubna, Russian Federation*³*Institute of Experimental Physics, Slovak Academy of Sciences, 040 14 Košice, Slovakia*⁴*Faculty of Science, Šafárik University, 040 01 Košice, Slovakia*⁵*Otto H. York Department of Chemical and Materials Engineering, New Jersey Institute of Technology, Newark, New Jersey 07102, USA*

(Received 2 February 2023; accepted 6 June 2023; published 27 June 2023)

The directed bond percolation is a paradigmatic model in nonequilibrium statistical physics. It captures essential physical information on the nature of continuous phase transition between active and absorbing states. In this paper, we study this model by means of the field-theoretic formulation with a subsequent renormalization group analysis. We calculate all critical exponents needed for the quantitative description of the corresponding universality class to the third order in perturbation theory. Using dimensional regularization with minimal subtraction scheme, we carry out perturbative calculations in a formally small parameter ε , where $\varepsilon = 4 - d$ is a deviation from the upper critical dimension $d_c = 4$. We use a nontrivial combination of analytical and numerical tools in order to determine ultraviolet divergent parts of Feynman diagrams.

DOI: [10.1103/PhysRevE.107.064138](https://doi.org/10.1103/PhysRevE.107.064138)**I. INTRODUCTION**

Nonequilibrium processes are prevalent in nature and the majority of observed phenomena are being in some form of nonequilibrium state [1,2]. Famous examples encompass turbulent flows [3], pattern formations [4], Earth's atmosphere [5], and living organisms [6]. A plethora of other examples can be found not only in the realm of physics and biology but also in chemistry, economy, sociology, climatology, and other research areas. The pervasiveness of the nonequilibrium systems raises the importance of their understanding, which is of utmost importance both for theoretical and practical applications. The past decades have witnessed rapid progress in the fundamental understanding of nonequilibrium physics.

Nonequilibrium systems are, from their very nature, dynamical and differ profoundly from systems that can be described as near-equilibrium models. Famous members of the latter group are all models of critical dynamics [7,8], which share a common property known as fluctuation-dissipation relation [9]. In genuine nonequilibrium systems, this relation is violated and the system is called far from equilibrium. Moreover, in order for a system to be in a nonequilibrium state, some mechanisms are necessary, which cause continuous doping of energy in and out of a system. This can be generated either by external means or by internal means as well.

From a whole set of possible nonequilibrium problems, an important collection is formed by growth models, which find a lot of applications in population dynamics, the creation of fractal structures, etc. From a theoretical point of view, such models can be described as stochastic systems in which the microscopic degrees of freedom evolve according to some probabilistic rules. The collective behavior of many microscopic entities usually allows us to employ continuum approximation in which certain nonuniversal properties, such as the type of a lattice structure, are absent.

Remarkably, despite the notorious difficulty of nonequilibrium models, they might simplify under specific circumstances and can be analytically tractable. We anticipate such simplification to occur when a dynamical system undergoes a continuous phase transition akin to equilibrium second-order phase transitions. At criticality, underlying degrees of freedom behave collectively over many spatiotemporal scales, which gives rise to self-similar scaling behavior. A particular hallmark is a large correlation length with respect to both time and spatial directions. In the critical region, it is then permissible [10,11] to approximate a system by means of the continuous or mesoscopic approach. Averaging small volumes whose diameter is much smaller than the correlation length leads to an effective description in terms of field variables. It is well known [11,12] that this enables us to use powerful methods of quantum (statistical) field theory. Further, many concepts and methods from equilibrium critical models can be taken over. One of the most important is the concept of universality class. According to it, systems can be categorized into different classes, whose members share the same macroscopic behavior. Completely different systems from a microscopic point of view could display the same critical behavior, which is determined to a great extent by some common gross

*hnatic@saske.sk

†m.kompaniets@spbu.ru

‡tomas.lucivjansky@upjs.sk

§mizisin@theor.jinr.ru

properties such as space dimension, symmetry, nature of order parameter, etc. All systems in the same universality class are quantitatively described by the same set of critical exponents. Therefore, to analyze their critical behavior it is advantageous to choose the simplest possible member of a given class.

Of particular importance is a group of dynamical models, whose phase space allows the existence of so-called absorbing states. These are such configurations that, once entered by a system, they cannot be left. The directed bond percolation (DP) process is probably the most common and famous paradigmatic model of fractal growth. Initially, it was developed [13] to model a spreading of fluid through an irregular porous medium in the presence of some external force, e.g., gravity. In biological terms, DP can be interpreted as a simple model for the epidemic process [14] in which there is no immunization of infected individuals. In the evolution of infectious diseases, sick individuals can spread infection to neighbors. The infected individuals are allowed to recover, but later the individuals can be sick again. The simple model exhibits a critical region between the state without the disease (the absorbing state) and the epidemic (the active state). Later, several other applications of DP have been found [15] in research areas as diverse as high energy physics [16,17], population dynamics [18], reaction-diffusion problems [19], contact process [20], forest fires models [21], a transition from laminar to turbulent flow [22–24], etc. Numerous other examples can be found in different models of physics, chemistry, biology, and even ecology [25].

Major attributes of the DP universality class are succinctly summarized by Janssen and Grassberger conjecture [26,27], according to which a system belongs to the DP universality class if four conditions are met: (i) the existence of the unique absorbing state, (ii) the positive one-component order parameter, (iii) short-range interactions, and (iv) no additional specific properties like quenched disorder or symmetries. Although this DP hypothesis has not been proven rigorously, yet strong support exists in its favor [15,28,29]. Systems fulfilling these conditions are expected to exhibit the same critical behavior. Similarly to equilibrium critical phenomena, nonequilibrium phase transition can be categorized into a different universality class [8,29], where systems within a given class display the same critical behavior. It might be claimed that the DP universality class plays a similar role in nonequilibrium dynamics as the Ising universal class in equilibrium systems [15].

Notwithstanding the fact that the DP universality class is quite robust, critical exponents were measured only in a few experiments during the past two decades. The DP phase transition was experimentally studied in turbulent liquid crystals [30,31], the transition from laminar to turbulent flow in channel flow [24,32], and in Couette flow [23]. Direct experimental verification is surprisingly low, especially as various possible experiments have been suggested in the past. Clearly, the experimental investigation of DP constitutes a formidable task for nonequilibrium physics.

Despite a lot of effort that has been put into a theoretical analysis of DP, even its simplest formulation in $(1+1)$ dimensions remains exactly unsolvable [29]. Typical theoretical approaches include numerical or approximate techniques such

as Monte Carlo, simulations, series expansions, diagonalization techniques, mapping on quantum spin chains, and others.

In this paper, we adopt a field-theoretic approach to study the universal properties of the directed percolation process. Though far from being the decisive approach to a problem, this method offers a great insight into the origin of universality and validation of scaling relations. Moreover, what is most relevant for this work is that it provides us with a calculation framework in which universal quantities can be calculated systematically. Our starting point is a mesoscopic formulation of DP, which further facilitates the use of a very powerful framework of the quantum field theory [11,33]. As observed by K. Wilson, critical systems, or more generally stochastic dynamical systems, can be interpreted as quantum field models in imaginary time, which facilitates the application of sophisticated methods from the quantum field theory.

First, we reformulate DP into a form of functional integral. Second, we calculate in a perturbative fashion relevant Green functions in the form of Feynman diagrams. Third, divergent diagrams are treated with a perturbative renormalization group (RG) in order to gain information about large-scale behavior. RG not only furnishes a conceptual formalism but also provides a powerful and versatile mechanism for computing universal quantities as critical exponents, amplitudes, and even perturbative calculation of scaling functions [9]. An important parameter in the RG procedure is the upper critical dimension d_c . It turns out that above d_c , the mean-field theory, which neglects fluctuations of the order parameter, predicts correct values for the critical exponents [9,11,34]. On the other hand, below d_c , fluctuations dominate behavior of the critical system and the mean-field approximation is not appropriate. More sophisticated approaches are called for. Precisely at the critical dimension d_c , RG theory predicts mean-field results with logarithmic corrections [9]. To now, the critical exponents have not been solved exactly below d_c , not even at spatial dimension $d = 1$. Traditionally, computer simulations are performed for the evaluation of critical exponents of the DP universality class, for instance, Monte Carlo simulation [29]. However, in past decades other lattice models were introduced that are members of the DP universality class, e.g., the Domany-Kinzel automaton or contact process [35]. Also, many numerical methods were developed as $(1+1)$ dimensional the low-density series expansion [36], the density matrix renormalization group method [37], nonperturbative renormalization group [38], and so on. The precision of critical exponents increases in lower space dimensions. However, in higher spatial dimensions below d_c , the error bars of computer simulations' results did not decrease substantially for many years of active research [8,29,39].

Within the field-theoretic renormalization group, a special role is played by dimensional regularization combined with ε expansion [9,10]. Using the former method, we can regularize divergent Feynman diagrams, whereas the latter is a convenient way in which physical expressions are calculated [9,10]. Formally, a small ε -expansion parameter is given by a difference $d_c - d$ from the upper critical dimension [as we will see later (Sec. III A) $d_c = 4$ for DP process]. The main quantitative results of RG are asymptotic series for critical exponents, and these have to be properly summed in order to

get precise numerical estimations [40]. Currently, analytical predictions for the critical exponents of DP universality class are known up to the second order of the perturbation theory [8,26,41,42]. The main aim of this paper is to substantially extend existing perturbative results up to the third order of perturbation theory in ε . To the best of our knowledge, this is the first time results with such precision are presented. Let us note that multiloop calculations usually represent a formidable task. Typically, perturbative calculations are feasible only for a small number of loops. The majority of calculations for nonequilibrium models are limited only to the two-loop approximation. The third-order perturbation theory thus poses a nontrivial improvement of existing results. It might be argued [43] that its severity is probably more than the order of magnitude worse than that of the second order. Not only is the number of Feynman diagrams much higher, but also there are numerical problems with the correct extraction of divergent parts of Feynman diagrams. In this paper, we combine both analytical and numerical techniques in order to calculate all necessary renormalization constants. We calculate Feynman diagrams numerically and then apply the field-theoretic RG method in an analytical fashion. Although some of the partial results have already been published previously [44–46], this paper contains analytical predictions for all critical exponents for the first time.

This paper is organized as follows. In Sec. II the field-theoretic formulation of DP process is presented. Renormalization group analysis is performed in Sec. III. Section IV describes nontrivial aspects of RG calculations in the third order of perturbation theory and Sec. V examines calculated predictions for critical exponents. Section VI is reserved for concluding remarks. The Supplemental Material [47] contains technical and numerical details about Feynman diagrams and their representation, algebraic structure, and divergent parts.

II. FIELD-THEORETIC FORMULATION OF DIRECTED PERCOLATION

A. Response functional

The effective field-theoretic model for directed percolation can be constructed in two different ways, which are completely equivalent with respect to universal large-scale behavior. The first approach starts with the microscopic version of the DP process on a lattice, which presents a specific reaction-diffusion system. Initially, the master equation [42] is introduced, whose final form is reformulated in terms of creation and annihilation operators using the Doi approach [48,49]. Finally, by means of coherent-state path integrals, one ends up with a field-theoretic action [8,42,50,51]. The second approach is based on phenomenological considerations supplemented by physical insights and symmetry considerations [29,42]. Both of the approaches are very well understood nowadays [8,29,42]. Thus we refrain here from giving a comprehensive derivation and briefly summarize the main aspects of the latter approach.

For DP the fundamental dynamic quantity is the density of active sites $\psi = \psi(t, \mathbf{x})$. Universal properties of the DP process in the critical region are then effectively captured by

the stochastic Langevin-like equation

$$\partial_t \psi = D_0 \nabla^2 \psi - D_0 \tau_0 \psi - \frac{D_0 g_0}{2} \psi^2 + \sqrt{\psi} \zeta, \quad (1)$$

where $\zeta = \zeta(t, \mathbf{x})$ denotes the noise field to be specified later, $\partial_t = \partial/\partial t$ is the time derivative, $\nabla^2 = \sum_{i=1}^d \partial/\partial x_i^2$ is the Laplace operator in d dimensions, D_0 is the diffusion constant, g_0 is the coupling constant, and τ_0 measures a deviation from the percolation threshold. For instance, for lattice DP [29] the $\tau = p_c - p$ is the deviation from a critical value probability p_c of open bonds, whereas, for laminar-turbulent phase transition [23,24,32], the $\tau = \text{Re} - \text{Re}_c$ is the deviation from a critical value of Reynolds number Re_c . In general, parameter τ plays an analogous role to the temperature variable $T - T_c$ in the paradigmatic φ^4 -theory in critical statics [9,10,42]. Factor $1/2$ has been added in front of the ψ^2 term for the future convenience.

RG procedure, which we employ, introduces two different kinds of variables—bare (unrenormalized) quantities and their renormalized counterparts. Therefore we denote the former ones with the subscript “0,” whereas the latter will be written without the subscript “0.” To keep the notation as simple as possible, bare functions (e.g., for connected Green functions) will be further denoted without the subscript “0” and their renormalized versions with the subscript R .

From the mathematical point of view, Eq. (1) should be interpreted in the Itô sense [52–55]. In detail, we assume that Gaussian noise field $\zeta(t, \mathbf{x})$ has zero mean $\langle \zeta \rangle = 0$ and correlations are given by the relation

$$\langle \zeta(t, \mathbf{x}) \zeta(t', \mathbf{x}') \rangle = g_0 D_0 \delta(t - t') \delta^{(d)}(\mathbf{x} - \mathbf{x}'), \quad (2)$$

where $\delta^{(d)}(\mathbf{x})$ is the d -dimensional Dirac delta function. Here brackets $\langle \dots \rangle$ denote averaging procedure over all possible realizations of the stochastic process. The multiplicative character of the noise in Eq. (1) can be regarded as a direct consequence of the absorbing condition, according to which all fluctuations have to cease once an absorbing state is entered.

In order to apply the RG method, it is advantageous to recast Langevin formulation (1) and (2) in terms of functional integrals. The stochastic problem (1) can be recast into a quantum-field model with a double set of fields [8,9,26]. Ensuing De Dominicis–Janssen dynamic functional of the percolation process [42,53,56] takes the following form:

$$\mathcal{S}(\varphi) = \int dx \left\{ \tilde{\psi} (-\partial_t + D_0 \nabla^2 - D_0 \tau_0) \psi + \frac{D_0 g_0}{2} (\tilde{\psi}^2 \psi - \tilde{\psi} \psi^2) \right\}, \quad (3)$$

where for brevity we write $x = (t, \mathbf{x})$ and integration measure as $dx = dt d^d x$, $\tilde{\psi}$ is an auxiliary Martin-Siggia-Rose response field, and $\varphi \equiv \{\psi, \tilde{\psi}\}$. Let us note that the response field $\tilde{\psi}$ arises from the integration over the noise ζ , and it might be interpreted as the functional Lagrange multiplier [8,9].

The existence of an additional symmetry in a quantum field model often provides additional invaluable information that might improve the tractability of theoretical analysis and practical calculations. The DP process possesses symmetry in

this sense, which is known in the literature as rapidity-reversal symmetry [15,29]. It can be directly observed that the action functional (3) is invariant with respect to the following transformation of fields ψ and $\tilde{\psi}$:

$$\psi(t, \mathbf{x}) \rightarrow -\tilde{\psi}(-t, \mathbf{x}), \quad \tilde{\psi}(t, \mathbf{x}) \rightarrow -\psi(-t, \mathbf{x}). \quad (4)$$

In Sec. III, we employ it to simplify the RG analysis.

B. Scale invariance

Dynamical models are characterized by two independent correlation lengths, besides the spatial length scale ξ_{\perp} there is also temporal length scale ξ_{\parallel} [8,9]. In the critical region, we thus expect that the introduced spatiotemporal scales diverge according to some power-law dependence,

$$\xi_{\perp} \sim |\tau_0|^{-\nu_{\perp}}, \quad \xi_{\parallel} \sim |\tau_0|^{-\nu_{\parallel}}, \quad (5)$$

where τ_0 was introduced in Eq. (1). Exponents ν_{\perp} and ν_{\parallel} take in Eq. (5) predominantly different values. In contrast to relativistic field theories (e.g., quantum electrodynamics), the models in statistical physics exhibit strong anisotropic scaling [8]. For a given dynamical universality class, it is then convenient to introduce the dynamical exponent z as a ratio,

$$z = \frac{\nu_{\parallel}}{\nu_{\perp}}. \quad (6)$$

In the scaling region, the correlation lengths are then simply related as $\xi_{\parallel} \sim \xi_{\perp}^z$.

There are two special values commonly encountered in physics $z = 1$ (light-cone spreading) and $z = 2$ (diffusive spreading). Values $z > 2$ correspond to a subdiffusive spreading, whereas $1 < z < 2$ to a superdiffusive spreading. As any other critical exponent z is an universal quantity.

For the full scaling description of DP process, one additional exponent is needed. Usually, this is the exponent β , which describes the mean particle number in the active phase,

$$\rho \sim (p - p_c)^{\beta} = (-\tau_0)^{\beta}. \quad (7)$$

C. Mean-field approximation

Arguably the most naive and direct approach to critical behavior is based on the mean-field (MF) theory, in which spatial variations of order parameter field are neglected [33]. Following this idea and neglecting the noise variable as well, we average Eq. (1) with an assumption $\langle \psi^2 \rangle \approx \langle \psi \rangle^2$. We immediately obtain an equation for the mean number of active sites $\rho(t) = \langle \psi \rangle$ in the form of an ordinary differential equation,

$$\frac{d\rho}{dt} = -D_0 \left(\tau_0 \rho + \frac{g_0}{2} \rho^2 \right). \quad (8)$$

Obviously, there are two stationary solutions to this equation $\rho_* = 0$ and $\rho_* = -2\tau_0/g_0$. The former corresponds to an absorbing state and is stable for $\tau_0 > 0$. On the other hand, the latter solution represents the active state realized for $\tau_0 < 0$. MF approach thus predicts phase transition at $\tau_0 = 0$.

From the theoretical point of view, MF theory is justified if the diffusive mixing of particles is much stronger than the influence of correlations produced by the reactions. However, computer simulations of DP reveal strong correlation effects

in the critical region, and therefore MF is inadequate and cannot yield precise quantitative results [29].

The spatially amended version of Eq. (8) is simply given by the deterministic partial differential equation,

$$\partial_t \psi = D_0 \nabla^2 \psi - D_0 \left(\tau_0 \psi + \frac{g_0}{2} \psi^2 \right), \quad (9)$$

where now order parameter field $\psi = \psi(t, \mathbf{x})$ depends also on a spatial variable. Direct scaling analysis [29] yields following values of critical exponents:

$$\nu_{\perp}^{\text{MF}} = \frac{1}{2}, \quad \nu_{\parallel}^{\text{MF}} = 1, \quad \beta^{\text{MF}} = 1. \quad (10)$$

III. RENORMALIZATION GROUP ANALYSIS

The main aim of the theory of critical behavior [10] is to understand how the nontrivial macroscopic (large-scale) behavior of the system might emerge from relatively simple microscopic interactions. Related quantitative analysis is usually accompanied by the determination of Green functions, i.e., correlation and response functions, as functions of the space-time coordinates. In the field-theoretic formulation, these functions can be represented in the form of perturbative sums, whose elements are conveniently expressed through Feynman diagrams. This formulation provides a convenient theoretical framework suitable for applying methods of statistical (quantum) field theory, among which the RG method plays a distinguished role. In particular, it facilitates a determination of the infrared (IR) asymptotic (large spatial and timescales) behavior of the Green functions, which is of fundamental importance for statistical physics. Feynman diagrams are often plagued with divergences, which have to be properly taken care of. In order to eliminate ultraviolet (UV) divergences renormalization procedure has to be applied [9,10]. There are various renormalization prescriptions available, each with its own advantages. In this work, we employ dimensional regularization supplemented with the minimal subtraction (MS) scheme. In this scheme, UV divergences manifest themselves in the form of poles in the small expansion parameters, which are given by a deviation from a critical dimension. A simplifying feature of MS scheme is the neglect of all finite parts of the Feynman graphs in the calculation of the renormalization constants. In the vicinity of critical points, large fluctuations on all spatiotemporal scales dominate the behavior of the system, which in turn results in the IR divergences in the Feynman graphs. The nontrivial connection between UV and IR divergences [8,9] for logarithmic theory allows us to derive RG differential equations, which describe scaling behavior. As a by-product, an analysis of these equations furnishes an efficient calculational technique for critical exponents.

The action Eq. (3) is amenable to the field-theoretic methods of quantum field theory [9]. Green functions correspond to functional averages with respect to the weight functional $\exp(S)$. In practical calculations, it is often more convenient to work preferably with connected Green functions. These correspond to Feynman diagrams that do not contain disconnected parts [9,10]. They can be obtained from the generating

functional \mathcal{W} ,

$$\mathcal{W}(A) = \ln \int \mathcal{D}\varphi \exp\{\mathcal{S}(\varphi) + \varphi A\}, \quad (11)$$

by taking the corresponding number of functional derivatives with respect to external sources $A = \{A_\psi, A_{\tilde{\psi}}\}$ at $A = 0$. Hereinafter, φ is the set $\{\psi, \psi'\}$ linear term in Eq. (11) is an abbreviated form for the following expression:

$$\varphi A \equiv \int dx [A_\psi(x)\psi(x) + A_{\tilde{\psi}}(x)\tilde{\psi}(x)]. \quad (12)$$

For translationally invariant theories, additional simplification consists in introducing functional $\Gamma(\alpha)$ for one-particle irreducible (1PI) Green functions [9,10]. This is an even more restricted class than that of connected Feynman diagrams, since 1PI diagrams are such diagrams that remain connected even after one internal line is cut [10,57]. It can be shown that the corresponding functional for 1PI diagrams [9] can be obtained by means of functional Legendre transform with respect to external sources A ,

$$\Gamma(\alpha) = W(A) - \alpha A, \quad \alpha(x) = \frac{\delta W(A)}{\delta A(x)}. \quad (13)$$

The independent argument for the functional Γ now becomes a pair of fields $\alpha = \{\alpha_\psi, \alpha_{\tilde{\psi}}\}$, while $A = A(\alpha)$ is implicitly determined by the second equation in Eq. (13). The 1PI Green functions $\Gamma^{(m,n)}$ are obtained by differentiation with respect to fields α ,

$$\Gamma^{(m,n)} \equiv \frac{\delta^{m+n}}{\delta \alpha_\psi^m \delta \alpha_{\tilde{\psi}}^n} \Gamma(\alpha) \Big|_{\alpha=0}. \quad (14)$$

As a result of causality, all 1PI Green functions of the form $\Gamma^{(0,n)}$ vanish. The same conclusion applies to related 1PI functions $\Gamma^{(m,0)}$ as a consequence of rapidity-reversal symmetry (4).

To abbreviate the notation, let us relabel variables α according to the prescription $\alpha \rightarrow \varphi$ and obtain an important relation [9,10] that summarizes the importance of generating functional for 1PI Feynman graphs in a concise manner,

$$\Gamma(\varphi) = \mathcal{S}(\varphi) + \Gamma_{\text{loop}}(\varphi), \quad (15)$$

where \mathcal{S} is the bare action functional of the model (3), and $\Gamma_{\text{loop}}(\varphi)$ is the sum of all 1PI loop diagrams contributions.

The starting point of perturbation methods in quantum field theory is to represent Green functions in terms of a corresponding sum of Feynman diagrams, whose relevance is controlled by interaction parameters (coupling constants). Feynman graphs represent convenient graphical representations of various algebraic structures that arise from basic perturbation elements, which are formed by propagators and interaction vertices.

For DP model, we encounter a single bare propagator, which is obtained from the quadratic part of the action functional (3). In a frequency-momentum representation, it reads

$$\langle \psi \tilde{\psi} \rangle_0(\omega, \mathbf{p}) = \frac{1}{-i\omega + \varepsilon_p}, \quad (16)$$

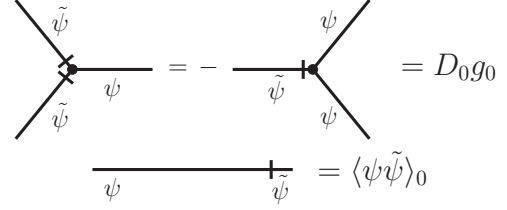


FIG. 1. Graphical representation of Feynman rules for DP model. The crossed line corresponds to a response field $\tilde{\psi}$.

where $\varepsilon_p = D_0(\mathbf{p}^2 + \tau_0)$. In time-momentum representation the propagator $\langle \psi \tilde{\psi} \rangle_0$ is given by

$$\langle \psi \tilde{\psi} \rangle_0(t, \mathbf{p}) = \theta(t) e^{-\varepsilon_p t}, \quad (17)$$

where $\theta(t)$ is the Heaviside step function.

Nonlinear terms in the action (3) generate two interaction vertices of the model, and they are associated with the vertex factors [9]

$$V_{\tilde{\psi}\psi\psi} = -V_{\tilde{\psi}\tilde{\psi}\psi} = D_0 g_0. \quad (18)$$

The Feynman rules for the DP model are depicted in Fig. 1 and, in fact, they represent the zero (tree) order of a perturbation theory [9]. Loop diagrams then contribute to higher-order terms with respect to the coupling constant g_0 , and as a rule, they exhibit various divergences in UV or IR sector. In graphical terms, these statements are part of Eq. (15). In particular, the two-point Green function takes the schematic form of the so-called Dyson equation

$$\Gamma^{(1,1)} = \langle \psi \tilde{\psi} \rangle_{1PI} = -\langle \psi \tilde{\psi} \rangle_0^{-1} + \text{diagram}, \quad (19)$$

where the shaded diagram corresponds to the loop corrections. Further, for the three-point interaction term, we have

$$\Gamma^{(1,2)} = \langle \psi \psi \tilde{\psi} \rangle_{1PI} = V_{\tilde{\psi}\psi\psi} + \text{diagram}. \quad (20)$$

The RG technique helps us to eliminate UV divergences, and through a nontrivial connection with IR behavior valid at the upper critical dimension, we can extract useful information about macroscopic behavior of universal quantities [8,9].

A. Canonical dimensions

The starting point of the actual RG analysis is a determination of canonical dimensions for all fields and parameters of the model [9,10]. As it has been pointed out in Sec. II B, DP process belongs to dynamical models and for such systems it is necessary to introduce two independent dimensions: a frequency dimension $d_\omega[Q]$ and a momentum dimension $d_k[Q]$, where Q is a given quantity (field or parameter) in the action functional (3). We employ standard normalization conditions

$$d_k[k] = -d_k[x] = 1, \quad d_k[\omega] = d_k[t] = 0, \quad (21)$$

$$d_\omega[k] = d_\omega[x] = 0, \quad d_\omega[\omega] = -d_\omega[t] = 1. \quad (22)$$

We aim to study the model in the asymptotic region $\omega \propto k^2$, which implies that both terms $\partial_t \psi$ and $\nabla^2 \psi$ are to be taken

TABLE I. Canonical dimensions of the bare fields and bare parameters for the action (3).

Q	ψ	$\tilde{\psi}$	D_0	τ_0	g_0
$d_\omega[Q]$	0	0	1	0	0
$d_k[Q]$	$d/2$	$d/2$	-2	2	$(4-d)/2$
$d[Q]$	$d/2$	$d/2$	0	2	$(4-d)/2$

on an equal footing. The total canonical dimension d_Q of a quantity Q is given by a weighted sum of momentum and frequency dimension,

$$d[Q] = d_k[Q] + 2d_\omega[Q]. \quad (23)$$

The canonical dimensions of all quantities (fields and parameters) in the DP action (3) are listed in Table I.

By usual considerations [9], we derive the formula for the total canonical dimension of an 1PI Green function Γ in the form

$$d[\Gamma^{(m,n)}] = d_k[\Gamma^{(m,n)}] + 2d_\omega[\Gamma^{(m,n)}]. \quad (24)$$

We can rewrite this equation with the help of Eq. (23) and Table I into a more informative form,

$$d[\Gamma^{(m,n)}] = d + 2 - nd[\psi] - md[\tilde{\psi}], \quad (25)$$

where n and m are a number of fields ψ and $\tilde{\psi}$ entering given Green function $\Gamma^{(m,n)}$.

As can be seen from Table I, the model is logarithmic at space dimension $d_c = 4$ when the coupling constant g_0 is dimensionless. In the dimensional regularization, it is reasonable to introduce a formally small parameter ε as a difference,

$$\varepsilon \equiv d_c - d = 4 - d. \quad (26)$$

For the logarithmic theory, the total canonical dimension $d[\Gamma]$ represents the formal degree of UV divergence, i.e.,

$$\delta_{(m,n)} = d[\Gamma^{(m,n)}]_{|\varepsilon=0}, \quad (27)$$

and UV divergences appear in a Green function as various poles in ε . The central step in the RG procedure lies in removing superficial UV divergences, which may appear only in those 1PI functions Γ for which UV index (27) δ_Γ attains non-negative values. In a straightforward manner, we determine that for DP model (3) the only 1PI functions with UV divergences are $\Gamma^{(1,1)}$, $\Gamma^{(2,1)}$, and $\Gamma^{(1,2)}$.

Green functions are, in perturbative calculations, naturally ordered in terms of a charge g_0 . As direct inspection of Feynman diagrams reveals, the actual charge of the perturbation theory is effectively g_0^2 rather than g_0 . Therefore it is advantageous to introduce a new charge u_0 as

$$u_0 = g_0^2, \quad (28)$$

with total canonical dimension $d[u_0] = \varepsilon$.

From the aforementioned considerations and taking into account symmetry (4), we infer that the renormalized action functional for the DP process can be written in the compact

form,

$$\mathcal{S}_R = \int dx \left\{ \tilde{\psi}_R (-Z_1 \partial_t + Z_2 D \nabla^2 - Z_3 D \tau) \psi_R + \frac{Dg}{2} Z_4 \mu^{\varepsilon/2} (\tilde{\psi}_R^2 \psi_R - \tilde{\psi}_R \psi_R^2) \right\}, \quad (29)$$

where $\psi_R, \tilde{\psi}_R$ are renormalized fields, μ is the reference mass scale in the MS scheme [9,10,34] with dimension $d[\mu] = 1$, and Z_i ($i = 1, 2, 3, 4$) are renormalization constants that need to be determined in a perturbative fashion. The fact that the interaction terms enter into the renormalization action as a single combination is a consequence of rapidity-reversal symmetry (4), i.e., nonlinear terms in the renormalized action (29) are renormalized with the same renormalization constant Z_4 . Therefore, in the actual calculations, we restrict our attention only to the 1PI Green function $\Gamma^{(2,1)}$.

Model (29) is multiplicatively renormalizable [8,26,42], and all UV divergences can be absorbed by the following renormalization prescription:

$$\psi = Z_\psi \psi_R, \quad \tilde{\psi} = Z_{\tilde{\psi}} \tilde{\psi}_R, \quad (30)$$

$$\tau_0 = Z_\tau \tau + \tau_c, \quad g_0 = \mu^{\varepsilon/2} Z_g g, \quad D_0 = Z_D D, \quad (31)$$

where Z_i ($i \in \{\psi, \tilde{\psi}, \tau, g, D\}$) are the corresponding renormalization constants. The term τ_c denotes the additive renormalization contribution (like a shift of a critical temperature T_c in the theory of critical behavior). Renormalization of the effective charge u directly follows from its definition (28)

$$u_0 = \mu^\varepsilon Z_u u, \quad Z_u = Z_g^2. \quad (32)$$

Clearly, renormalized charge u is dimensionless.

Relations between the renormalization constants for fields and parameters and renormalization constants Z_i ; $i = 1, 2, 3, 4$ can be deduced straightforwardly from the renormalized action (29),

$$Z_1 = Z_\psi Z_{\tilde{\psi}}, \quad (33)$$

$$Z_2 = Z_D Z_\psi Z_{\tilde{\psi}}, \quad (34)$$

$$Z_3 = Z_\tau Z_D Z_\psi Z_{\tilde{\psi}}, \quad (35)$$

$$Z_4 = Z_g Z_D Z_\psi^2 Z_{\tilde{\psi}}^2 = Z_g Z_D Z_\psi Z_{\tilde{\psi}}^2. \quad (36)$$

Inverting these relations yields

$$Z_\psi = Z_{\tilde{\psi}} = Z_1^{1/2}, \quad (37)$$

$$Z_D = Z_2 Z_1^{-1}, \quad (38)$$

$$Z_u = Z_g^2 = Z_4 Z_2^{-2} Z_1^{-1}, \quad (39)$$

$$Z_\tau = Z_3 Z_2^{-1}, \quad (40)$$

where the first equality is a consequence of symmetry (4).

In actual calculations, we thus need to concentrate solely on an analysis of renormalization constants Z_i , where $i = 1, 2, 3, 4$.

two-loop diagrams

$$\frac{1}{2} \left[\text{diagram 1} + \text{diagram 2} \right], \quad (54)$$

and, finally, the most important contributions to our aim are summarized by a following sum of three-loop Feynman diagrams

$$\begin{aligned} & \text{diagram 1} + \text{diagram 2} \\ & + \text{diagram 3} + \text{diagram 4} \\ & + \text{diagram 5} + \frac{1}{4} \text{diagram 6} \\ & + \frac{1}{8} \text{diagram 7} + \frac{1}{2} \text{diagram 8} \\ & + \frac{1}{2} \text{diagram 9} + \text{diagram 10} \\ & + \text{diagram 11} + \frac{1}{2} \text{diagram 12} \\ & + \frac{1}{2} \text{diagram 13} + \frac{1}{2} \text{diagram 14} \\ & + \frac{1}{2} \text{diagram 15} + \frac{1}{2} \text{diagram 16} \\ & + \text{diagram 17} \end{aligned} \quad (55)$$

The function $\Gamma^{(1,2)}$ in the one-loop approximation corresponds to a single triangle-like Feynman

graph

$$\text{triangle diagram} \quad (56)$$

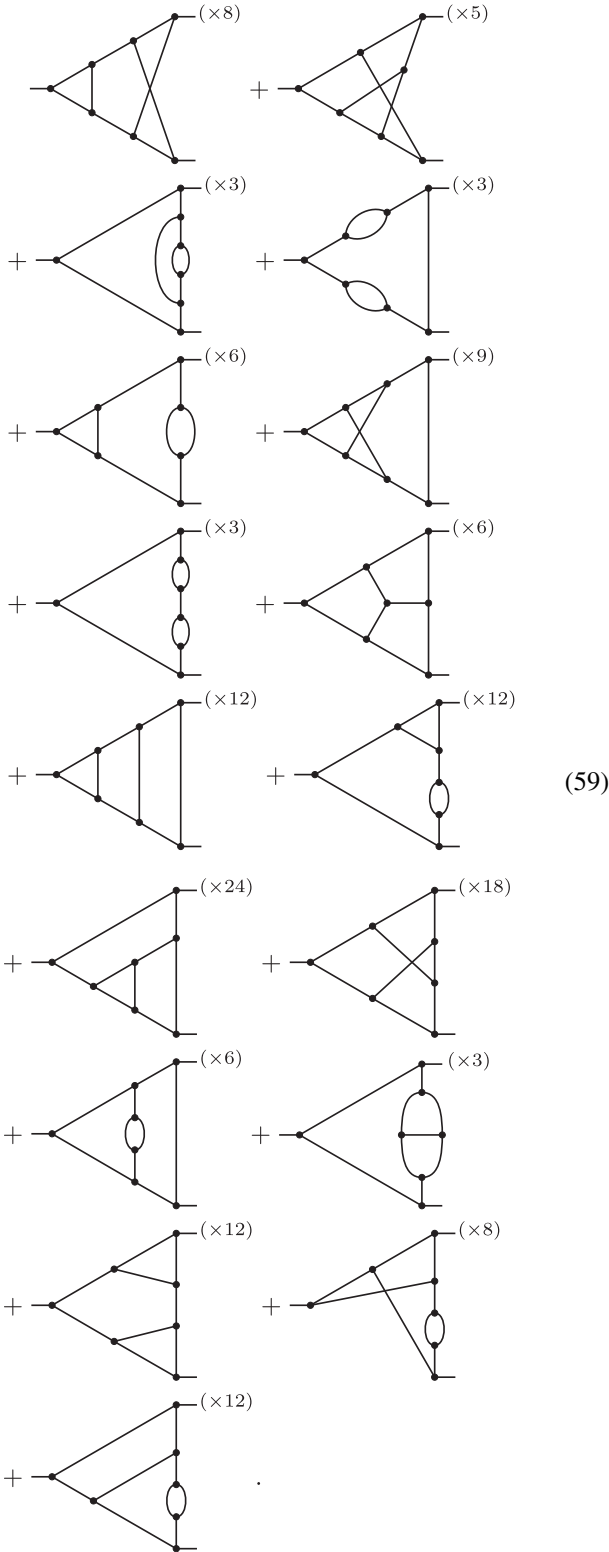
In the two-loop approximation, there are altogether three distinct graph topologies (skeleton diagrams)

$$\begin{aligned} & (\times 6) \text{diagram 1} + (\times 3) \text{diagram 2} \\ & + (\times 2) \text{diagram 3} \end{aligned} \quad (57)$$

where to make the notation more compact we have not explicitly denoted response fields as introduced in graphical rules from Fig. 1. Instead, we have explicitly written a numerical factor after a diagram, which corresponds to its multiplicity. For a given diagram, it is then straightforward to reconstruct needed configurations of response field $\tilde{\psi}$. For example, the second graph at the two-loop approximation (57) corresponds to

$$\begin{aligned} & (\times 3) \text{diagram 1} = \text{diagram 1} \\ & + \text{diagram 2} + \text{diagram 3} \end{aligned} \quad (58)$$

Last, the three-loop approximation comprises the following graph topologies:



A computer algorithm for the calculation of Feynman diagrams is similar to that of model A [58]; it generalizes the original Sector Decomposition algorithm [59] to the models of critical dynamics. For actual numerical calculations, we have applied the Vegas algorithm from CUBA library with a new

TABLE II. The number of Feynman diagrams for DP model that need to be analyzed for the three-loop approximation.

Diagrams	One-loop	Two-loop	Three-loop
$\langle \tilde{\psi} \psi \rangle$	1	2	17
$\langle \tilde{\psi} \psi \psi \rangle$	1	11	150

implementation [60]. Altogether, the number of needed Feynman diagrams in three-loop approximation is much higher than in the two-loop approximation (see Table II), which makes the problem technically more involved. Results for coefficients $\Gamma_i^{(k)}$ read

$$\Gamma_1^{(1)} = \frac{1}{8\epsilon} - \frac{1}{16} + \frac{\pi^2\epsilon}{192}, \quad (60)$$

$$\Gamma_1^{(2)} = \frac{7}{128\epsilon^2} - 0.053082575(5)\frac{1}{\epsilon} + 0.041287893(4), \quad (61)$$

$$\Gamma_1^{(3)} = \frac{91}{3072\epsilon^3} - 0.0359754(2)\frac{1}{\epsilon^2} + 0.0226904(4)\frac{1}{\epsilon}, \quad (62)$$

$$\Gamma_2^{(1)} = \frac{1}{16\epsilon} - \frac{1}{32} + \frac{\pi^2\epsilon}{384}, \quad (63)$$

$$\Gamma_2^{(2)} = \frac{13}{512\epsilon^2} - 0.02594616442(3)\frac{1}{\epsilon} + 0.020722022(2), \quad (64)$$

$$\Gamma_2^{(3)} = \frac{325}{24576\epsilon^3} - 0.01710044(3)\frac{1}{\epsilon^2} + 0.01059489(8)\frac{1}{\epsilon}, \quad (65)$$

$$\Gamma_3^{(1)} = \frac{1}{4\epsilon} - \frac{1}{8} + \frac{\pi^2\epsilon}{96}, \quad (66)$$

$$\Gamma_3^{(2)} = \frac{1}{8\epsilon^2} - \frac{7}{64\epsilon} + 0.07874750(3), \quad (67)$$

$$\Gamma_3^{(3)} = \frac{325}{24576\epsilon^3} - 0.0765338(3)\frac{1}{\epsilon^2} + 0.0430058(6)\frac{1}{\epsilon}, \quad (68)$$

$$\Gamma_4^{(1)} = \frac{1}{2\epsilon} - \frac{1}{4} + \frac{\pi^2\epsilon}{48}, \quad (69)$$

$$\Gamma_4^{(2)} = \frac{5}{16\epsilon^2} - \frac{1}{4\epsilon} + 0.17227563(2), \quad (70)$$

$$\Gamma_4^{(3)} = \frac{5}{24\epsilon^3} - 0.1921389(7)\frac{1}{\epsilon^2} + 0.098458(2)\frac{1}{\epsilon}. \quad (71)$$

From these expressions, we obtain RG constants $Z_1 - Z_4$ to the three-loop approximation in a straightforward manner,

$$Z_1 = 1 + \frac{u}{8\epsilon} + u^2 \left[\frac{7}{128\epsilon^2} - 0.013323675(6)\frac{1}{\epsilon} \right] + u^3 \left[\frac{91}{3072\epsilon^3} - 0.024562(2)\frac{1}{\epsilon^2} + 0.0051821(5)\frac{1}{\epsilon} \right], \quad (72)$$

$$Z_2 = 1 + \frac{u}{16\epsilon} + u^2 \left[\frac{13}{512\epsilon^2} - 0.0053038358(4)\frac{1}{\epsilon} \right] + u^3 \left[\frac{325}{24576\epsilon^3} - 0.01110090(3)\frac{1}{\epsilon^2} + 0.00072908(8)\frac{1}{\epsilon} \right], \quad (73)$$

$$\begin{aligned}
Z_3 &= 1 + \frac{u}{4\varepsilon} + u^2 \left[\frac{1}{8\varepsilon^2} - \frac{5}{128\varepsilon} \right] \\
&\quad + u^3 \left[\frac{7}{96\varepsilon^3} - 0.0617665(3) \frac{1}{\varepsilon^2} + 0.0253140(6) \frac{1}{\varepsilon} \right], \\
Z_4 &= 1 + \frac{u}{2\varepsilon} + u^2 \left[\frac{5}{16\varepsilon^2} - \frac{7}{64\varepsilon} \right] \\
&\quad + u^3 \left[\frac{5}{24\varepsilon^3} - 0.1743138(7) \frac{1}{\varepsilon^2} + 0.0888244(15) \frac{1}{\varepsilon} \right].
\end{aligned} \tag{74}$$

Complete diagram-by-diagram results are summarized in the Supplemental Material [47]. Feynman diagrams were encoded using efficient scheme based on so-called Nickel index [61–63]. In Appendix, we also give additional relations between diagrams that were used as an additional crosscheck.

In a straightforward manner, it is possible to calculate corresponding expressions for renormalization constants for parameters and fields introduced in Eqs. (30) and (31). Their explicit forms read

$$\begin{aligned}
Z_\psi &= 1 + \frac{u}{16\varepsilon} + u^2 \left[0.02539062504(4) \frac{1}{\varepsilon^2} - 0.006661838(3) \frac{1}{\varepsilon} \right] \\
&\quad + u^3 \left[0.01322428(3) \frac{1}{\varepsilon^3} - 0.01186460(8) \frac{1}{\varepsilon^2} + 0.0025911(2) \frac{1}{\varepsilon} \right],
\end{aligned} \tag{76}$$

$$\begin{aligned}
Z_D &= 1 - \frac{u}{16\varepsilon} + u^2 \left[-0.02148437507(9) \frac{1}{\varepsilon^2} + 0.008019839(5) \frac{1}{\varepsilon} \right] \\
&\quad + u^3 \left[-0.01029458(5) \frac{1}{\varepsilon^3} + 0.0116260(2) \frac{1}{\varepsilon^2} - 0.0044531(5) \frac{1}{\varepsilon} \right],
\end{aligned} \tag{77}$$

$$\begin{aligned}
Z_\tau &= 1 + \frac{3u}{16\varepsilon} + u^2 \left[0.0878906250(2) \frac{1}{\varepsilon^2} - 0.033758658(11) \frac{1}{\varepsilon} \right] \\
&\quad + u^3 \left[0.04943859(6) \frac{1}{\varepsilon^3} - 0.0475612(2) \frac{1}{\varepsilon^2} + 0.0245840(6) \frac{1}{\varepsilon} \right],
\end{aligned} \tag{78}$$

$$Z_u = 1 + \frac{3u}{4\varepsilon} + u^2 \left[\frac{9}{16\varepsilon^2} - 0.19481863(3) \frac{1}{\varepsilon} \right] + u^3 \left[0.4218749(3) \frac{1}{\varepsilon^3} - 0.3409311(13) \frac{1}{\varepsilon^2} + 0.171009(3) \frac{1}{\varepsilon} \right]. \tag{79}$$

B. RG equation

We have been able to determine RG constants in the MS scheme up to the third order in perturbation theory. In the calculation process itself, we have used various verification procedures in order to avoid any conceivable errors. All relevant information regarding each of the three-loop Feynman diagrams can be found in the Supplemental Material [47].

Once the calculation of RG constants is successfully accomplished, we are in a position to analyze the asymptotic behavior of experimentally measurable quantities, in particular, critical exponents. These govern scaling properties of the DP model [15,29] in the critical region $\tau \rightarrow 0$. Although many permissible Green functions might be studied, here we focus on the simplest nontrivial functions. As a result, we obtain numerical predictions for critical exponents. Additional work would be needed for a calculation of universal moment ratios [29], and a much more demanding task would be a RG analysis of so-called scaling functions [64].

In order to derive basic RG differential equations, let us introduce a differential operator

$$\tilde{D}_\mu \equiv \mu \partial_\mu |_0, \tag{80}$$

where $\partial_\mu |_0$ is the corresponding derivative at fixed bare parameters. Applying it to Eq. (48) yields the basic RG differ-

ential equations [9,34] for renormalized 1PI Green functions

$$(\tilde{D}_\mu - n\gamma_\psi - m\gamma_{\tilde{\psi}}) \Gamma_R^{(m,n)}(\dots; e, \mu) = 0. \tag{81}$$

For the DP model, the differential operator \tilde{D}_μ can be expressed through renormalized variables as follows

$$\tilde{D}_\mu = \mu \partial_\mu + \beta_u \partial_u - \tau \gamma_\tau \partial_\tau - D \gamma_D \partial_D. \tag{82}$$

Here β_u is the beta function of the coupling constant u , and γ_Q ; $Q \in \{\psi, \tilde{\psi}, D, \tau\}$ are anomalous dimensions for fields and parameters. They are defined [9,10] as

$$\gamma_Q \equiv \mu \partial_\mu |_0 \ln Z_Q. \tag{83}$$

In a straightforward fashion, this relation can be rewritten into a more useful form,

$$\gamma_Q = -\varepsilon \frac{u \partial_u \ln Z_Q}{1 + u \partial_u \ln Z_u}, \tag{84}$$

by which the anomalous dimension is expressed solely in terms of renormalized variables. The beta function β_u governs the RG flow of the theory, and DP process is an example of the single charge theory. Hence, we only have to deal with one beta function,

$$\beta_u \equiv \mu \partial_\mu |_0 u. \tag{85}$$

Using similar considerations as for an anomalous dimension in Eq. (84) and relation (32) we can express the beta function β_u in two different ways,

$$\beta_u = -u(\varepsilon + \gamma_u) \quad (86)$$

$$= -\varepsilon \frac{u}{1 + u\partial_u \ln Z_u}. \quad (87)$$

Final predictions for the anomalous dimensions take the following form:

$$\gamma_\psi = -\frac{u}{16} + 0.013323675(5)u^2 - 0.0077732(7)u^3, \quad (88)$$

$$\gamma_D = \frac{u}{16} - 0.016039678(11)u^2 + 0.0133592(13)u^3, \quad (89)$$

$$\gamma_\tau = -\frac{3u}{16} + 0.06751732(2)u^2 - 0.073755(2)u^3, \quad (90)$$

$$\gamma_u = -\frac{3u}{4} + 0.38963725(5)u^2 - 0.513026(9)u^3, \quad (91)$$

where the number in brackets corresponds to a numerical error stemming from applied integration procedures. As can be directly seen in expressions (88)–(91), the obtained results display a high level of accuracy.

Finally, the beta function β_u takes in the three-loop approximation form

$$\beta_u = -u \left[\varepsilon - \frac{3u}{4} + 0.38963725(5)u^2 - 0.513026(9)u^3 \right]. \quad (92)$$

Expressions (88)–(92) can be regarded as the most important results of this paper. To the best of our knowledge, this is the first time field-theoretical predictions for three-loop corrections are presented for a nonequilibrium model.

V. DIRECTED PERCOLATION UNIVERSALITY CLASS

The existence of an IR attractive fixed point ensures the scaling behavior of theory [9,34]. The asymptotic behavior is then governed by IR attractive fixed points of corresponding RG equations. The coordinates of fixed points can be found from the requirement that all beta functions of a model simultaneously vanish,

$$\beta_i(g^*) = 0, \quad \beta_i = \mu\partial_{\mu}|_0 g_i, \quad (93)$$

where g_i are charges of the theory. IR stability of fixed points is determined from a matrix Ω of the first derivatives with respect to coupling constants $\Omega_{ij} = \partial\beta_{g_i}/\partial g_j$. A fixed point is IR attractive when all eigenvalues of Ω are positive.

For DP process, a stability analysis is straightforward as we have to deal with a single beta function β_u . Hence, to determine the stability of given fixed points only one derivative $\partial\beta_u/\partial u$ is needed. From the standard requirements imposed on an IR attractive fixed point, the DP process reveals two possible solutions: the trivial (Gaussian) fixed point ($u^* = 0$) corresponds to a mean-field solution, whereas the nontrivial fixed point is given by the following approximate coordinate,

$$u^* = \frac{4\varepsilon}{3} + 0.92358460(12)\varepsilon^2 - 0.34190(3)\varepsilon^3. \quad (94)$$

The Gaussian fixed point is IR attractive for $\varepsilon < 0$, which according to Eq. (26) corresponds to higher space dimensions

$d > d_c$. On the other hand, the nontrivial fixed point is IR stable for $\varepsilon > 0$, which corresponds to physically more relevant space dimensions $d < 4$.

The existence of IR solution of RG equations implies the scaling behavior of Green functions. From the macroscopic point of view, the parameters of the model can be divided into two groups: IR irrelevant quantities (D , g , u , and μ) and IR relevant (momenta and coordinates, frequency and time, and τ and fields). For a dynamical model [9], the critical dimension of the IR relevant quantity Q is given by the general formula

$$\Delta_Q = d_k[Q] + \Delta_\omega d_\omega[Q] + \gamma_Q^*, \quad (95)$$

where the critical dimension of frequency Δ_ω is related to the anomalous dimension γ_D by

$$\Delta_\omega = 2 - \gamma_D^*. \quad (96)$$

Normalization conditions are assumed in the form

$$\Delta_k = -\Delta_x = 1, \quad (97)$$

and $d_k[Q]$ and $d_\omega[Q]$ in Eq. (95) denote canonical dimensions of quantity Q (see Table I), γ_Q^* is the value of anomalous dimension at the given fixed point. The remaining relevant critical dimensions can be expressed through critical anomalous dimensions γ_ψ^* and γ_τ^* ,

$$\Delta_{\psi'} = \Delta_\psi = \frac{d}{2} + \gamma_\psi^*, \quad \Delta_\tau = 2 + \gamma_\tau^*. \quad (98)$$

Due to a rapidity-reversal symmetry (4), only three critical dimensions are thus sufficient to fully describe DP universality class.

A. Critical exponents

In contrast to multiscaling problems [9,65], such as turbulence, the DP universality class is an example of theory exhibiting simple scaling behavior. This amounts to that only finite numbers of independent exponents are necessary to describe unambiguously DP universality class.

In lower space dimensions $d \leq 2$ theoretical analysis is intricate as infrared singularities are encountered $\varepsilon = 2$ ($d = 2$), and they cannot be dealt by RG method [42]. On the other hand, for the most realistic three-dimensional DP process, which corresponds to $\varepsilon = 1$ ($d = 3$), many results from numerical simulations are available nowadays. They exhibit an even higher level of inaccuracy and field-theoretic predictions seem to provide the most reliable estimates.

In order to describe DP process quantitatively, let us introduce appropriate quantities. As the most relevant appears the density of active particles $n(t)$ at time t averaged over the entire system, which can be regarded as the order parameter of DP. In active state density, $n(t)$ is expected to scale in an asymptotic limit $t \rightarrow \infty$ according to a power law,

$$n(\infty) \sim |\tau|^\beta. \quad (99)$$

The scaling behavior of several other quantities can be derived from the two-point Green function. Both from a practical and theoretical points of view a special role is played by the response function $W_{\psi\tilde{\psi}} = \langle \psi(t, \mathbf{x}) \tilde{\psi}(0, \mathbf{0}) \rangle$. Its scaling form

can take various forms. For our purposes here, they are given by

$$W_{\psi\bar{\psi}}(t, \mathbf{x}, \tau) = t^{-2\Delta_\psi/\Delta_\omega} f\left(\frac{\mathbf{x}}{t^{1/\Delta_\omega}}, \frac{\tau}{t^{-\Delta_\tau/\Delta_\omega}}\right), \quad (100)$$

$$W_{\psi\bar{\psi}}(t, \mathbf{x}, \tau) = |\tau|^{2\Delta_\psi/\Delta_\tau} g\left(\frac{t}{|\tau|^{-\Delta_\omega/\Delta_\tau}}, \frac{\mathbf{x}}{|\tau|^{-1/\Delta_\tau}}\right), \quad (101)$$

where we have taken into account the relation $\Delta_t = -\Delta_\omega$. In DP lattice models [29] the response function is used in order to define quantities such as the number of active sites $N(t, \tau)$ generated from the origin

$$N(t, \tau) = \int d^d x W_{\psi\bar{\psi}}(t, \mathbf{x}, \tau), \quad (102)$$

which are crucial for seed simulations.

At criticality, the number of active particles displays asymptotic power-law behavior governed by the critical exponent θ . Substituting Eq. (100) into the definition for $N(t)$ we derive the following scaling form:

$$N(t, \tau) = t^{(d-2\Delta_\psi)/\Delta_\omega} F(\tau t^{\Delta_\tau/\Delta_\omega}), \quad (103)$$

where the scaling function F is finite at the critical point $\tau = 0$. The critical exponent θ is defined in terms of critical dimensions in the following way:

$$\theta \equiv \frac{d - 2\Delta_\psi}{\Delta_\omega}. \quad (104)$$

We then arrive at a three-loop prediction (the third order in the expansion parameter ε),

$$\theta = \frac{\varepsilon}{12} + 0.037509726(13)\varepsilon^2 - 0.032978(3)\varepsilon^3. \quad (105)$$

Another dynamical quantity is the mean-square radius $R^2(t)$ of spreading particles starting from a single seed at the origin at time $t = 0$ [29,42]. It is defined by

$$R^2(t, \tau) \equiv \frac{\int d^d x \mathbf{x}^2 W_{\psi\bar{\psi}}(t, \mathbf{x}, \tau)}{\int d^d x W_{\psi\bar{\psi}}(t, \mathbf{x}, \tau)}. \quad (106)$$

In a similar way as has been done for $n(t, \tau)$ we can obtain the asymptotic scaling behavior for R^2 in criticality,

$$R^2 \sim t^{2/z}, \quad (107)$$

where the dynamical exponent z in our notation is equal to the critical exponent of frequency, i.e., $z = \Delta_\omega$.

A two-loop calculation for z can be performed in an analytical fashion [26,41,42] with the final perturbative prediction,

$$z = 2 - \frac{\varepsilon}{12} - \left(\frac{67}{288} + \frac{59}{144} \ln \frac{4}{3}\right) \frac{\varepsilon^2}{12}. \quad (108)$$

The corresponding value to the third order in perturbation theory is determined from the relation (95) and reads

$$z = 2 - \frac{\varepsilon}{12} - 0.02920905(2)\varepsilon^2 + 0.029207(4)\varepsilon^3. \quad (109)$$

A further quantity, which elucidates the nature of DP universality class, is the mean cluster mass M , which is also related to the two-point connected Green function [29],

$$M(\tau) = \int d^d x \int_0^\infty dt W_{\psi\bar{\psi}}(\mathbf{x}, t, \tau). \quad (110)$$

TABLE III. Critical exponents of DP universality class. More details can be found in the literature [8,15,29,42].

Observable	Exponent	Asymptotic relation
Order parameter	$\beta = \frac{\Delta_\psi}{\Delta_\tau}$	$n(\tau, t \rightarrow \infty) \sim \tau ^\beta$
	$\alpha = \frac{\Delta_\psi}{\Delta_\omega}$	$n(\tau = 0, t) \sim t^{-\alpha}$
Survival probability	$\beta' = \beta$	$P(\tau, t \rightarrow \infty) \sim \tau ^{\beta'}$
	$\delta = \alpha$	$P(\tau = 0, t) \sim t^{-\delta}$
Mean-square radius	$z = \Delta_\omega$	$R^2(\tau = 0, t) \sim t^{2/z}$
Correlation length	$\nu_\perp \equiv \nu = \frac{1}{\Delta_\tau}$	$\xi(\tau, t \rightarrow \infty) \sim \tau ^{-\nu_\perp}$
	$\nu_\parallel \equiv z\nu = \frac{\Delta_\omega}{\Delta_\tau}$	$\xi(\tau, t \rightarrow \infty) \sim \tau ^{-\nu_\parallel}$
Number of active sites	$\theta = \frac{d-2\Delta_\psi}{\Delta_\omega}$	$N(\tau = 0, t) \sim t^\theta$
Mean cluster mass	$\gamma = \frac{d+\Delta_\omega-2\Delta_\psi}{\Delta_\tau}$	$M(\tau, t \rightarrow \infty) \sim \tau ^{-\gamma}$
Mean size of cluster	$\sigma = \frac{d+\Delta_\omega-\Delta_\psi}{\Delta_\tau}$	$S(\tau, t \rightarrow \infty) \sim \tau ^{-\sigma}$

Substituting the asymptotic formula (101) into this definition and rescaling the time and space variables accordingly leads to the asymptotic power-law behavior,

$$M(\tau) \propto |\tau|^{-(d+\Delta_\omega-2\Delta_\psi)/\Delta_\tau}, \quad (111)$$

where additional scaling dependence has been suppressed. The definition of the exponent γ directly follows

$$\gamma = \frac{d + \Delta_\omega - 2\Delta_\psi}{\Delta_\tau}. \quad (112)$$

From our three-loop calculation, we obtain the following result:

$$\gamma = 1 + \frac{\varepsilon}{6} + 0.06683697(2)\varepsilon^2 - 0.036156(4)\varepsilon^3. \quad (113)$$

As has already been mentioned, a complete description of the DP universality class requires knowledge of exactly three independent critical exponents. Customarily [8,29], the triple $(\beta, \nu_\parallel, \nu_\perp)$ is chosen. Our calculation shows that to the three-loop approximation they are given by

$$\beta = 1 - \frac{\varepsilon}{6} - 0.01128142(2)\varepsilon^2 - 0.015743(3)\varepsilon^3, \quad (114)$$

$$\nu_\parallel = 1 + \frac{\varepsilon}{12} + 0.02238280(2)\varepsilon^2 - 0.008169(3)\varepsilon^3, \quad (115)$$

$$\nu_\perp = \frac{1}{2} + \frac{\varepsilon}{16} + 0.021097832(11)\varepsilon^2 - 0.009594(2)\varepsilon^3. \quad (116)$$

Additional relations and definitions of critical exponents are summarized in Table III and take the following form:

$$\alpha = 1 - \frac{\varepsilon}{4} - 0.012830892(11)\varepsilon^2 - 0.000910(2)\varepsilon^3, \quad (117)$$

$$\sigma = 2 + \frac{\varepsilon^2}{18} - 0.051899(8)\varepsilon^3. \quad (118)$$

The critical exponents can be directly compared to previous analytical results [26,42] calculated to the two-loop

TABLE IV. Evaluation of critical exponents of DP universality class in three space dimensions $\varepsilon = 1$ ($d = 3$): Padé approximant (P_D^N), Padé resummation, Direct summation, results from Monte Carlo simulations of the contact process and nonperturbative renormalization group. The symbol * marks value that was calculated using scaling relations [15]. The first two rows correspond to Padé approximants [66,67] calculated from our two-loop and three-loop results, respectively.

	$\beta = \beta'$	ν_{\perp}	ν_{\parallel}	$\alpha = \delta$	γ	z	θ	σ
Padé (two-loop)	0.833(17)	0.580(15)	1.101(15)	0.76(3)	1.23(5)	1.90(2)	0.12(6)	2.04(6)
Padé (three-loop)	0.818(10)	0.581(8)	1.103(6)	0.740(6)	1.23(3)	1.898(14)	0.11(4)	2.03(2)
Ref. [39]	0.813(11)	0.584(6)*	1.11(1)	0.732(4)	1.23(3)*	1.901(5)*	0.114(4)	2.05(4)*
Ref. [35]	0.815(2)	0.5826(9)	1.106(2)	0.7367(6)	1.224(5)*	1.8986(8)	0.1062(4)	2.039(4)*
Ref. [68]	0.809(3)*	0.580(2)*	1.114(4)	0.7263(11)	1.237(6)*	1.919(4)*	0.110(1)	2.046(8)*
Ref. [69]	0.818(4)	0.582(2)	1.106(3)	0.7398(10)	1.216(10)*	1.8990(4)	0.1057(3)	2.034(8)*
Ref. [38]	0.782	0.548	1.046*	0.747*	1.126*	1.909	0.0764*	1.908*

approximation (the second order in ε),

$$\beta = 1 - \frac{\varepsilon}{6} + \left(\frac{11}{12} - \frac{53}{6} \ln \frac{4}{3} \right) \frac{\varepsilon^2}{144}, \quad (119)$$

$$\nu_{\parallel} = 1 + \frac{\varepsilon}{12} + \left(\frac{109}{24} - \frac{55}{12} \ln \frac{4}{3} \right) \frac{\varepsilon^2}{144}, \quad (120)$$

$$\nu_{\perp} = \frac{1}{2} + \frac{\varepsilon}{16} + \left(\frac{107}{32} - \frac{17}{16} \ln \frac{4}{3} \right) \frac{\varepsilon^2}{144}. \quad (121)$$

Their numerical evaluation yields the following expressions:

$$\beta = 1 - \frac{\varepsilon}{6} - 0.0112814234\varepsilon^2, \quad (122)$$

$$\nu_{\parallel} = 1 + \frac{\varepsilon}{12} + 0.0223828044\varepsilon^2, \quad (123)$$

$$\nu_{\perp} = \frac{1}{2} + \frac{\varepsilon}{16} + 0.0210978319\varepsilon^2, \quad (124)$$

which agrees very well with our results (114)–(116).

In the numerical calculation, there is a nontrivial way to verify the numerical values of critical exponents. This is based on a generalized hyperscaling relation [15], which takes the form

$$\theta - \frac{d}{z} = -\frac{\beta + \beta'}{\nu_{\parallel}}. \quad (125)$$

However, this relation is automatically fulfilled once critical exponents are expressed in terms of critical dimensions.

Another possibility would be to compare numerical results to predictions obtained by Monte Carlo simulations on a lattice in a certain space dimension [29].

B. Resummation results

It is well known [10] that typical perturbative series in quantum (statistical) field theory [such as expressions for critical exponents (114)–(116)] are asymptotic rather than convergent. There exist powerful mathematical methods suitable for their analysis [40], which might extract useful physical information. Therefore, it is reasonable to apply some summation on the part of an asymptotic series. In order to attain progress, we apply resummation techniques and compare obtained results.

The final results of critical exponents are calculated as an asymptotic series in formally small $\varepsilon = 4 - d$. To obtain

final values in the physically relevant space dimension $d = 3$ ($\varepsilon = 1$) we use Padé approximants with the strategy described in Refs. [66,67]. These values of critical exponents can be found in Table IV, where they are compared with the results from Monte Carlo simulation for the contact process [35,39] and with results obtained from the high-precision Monte Carlo analysis [68,69]. The latter belongs to the DP universality class, and calculated critical exponents are in agreement within corresponding error bars.

VI. CONCLUSION

In this paper, we have calculated the critical exponents of DP universality class up to the third order of perturbation theory. We have formulated DP process within the field-theoretic framework and performed a full UV renormalization analysis. We have limited ourselves to compute only three critical exponents needed for a description of the DP process. In particular, we have found perturbative ε expansion for three independent critical exponents β , ν_{\perp} , ν_{\parallel} (or θ , z , γ) to the third order in ε . Our results are in agreement with the two-loop analytic calculations.

In calculation of the RG constants, we have identified three distinguished properties, which has helped us simplify difficult technical part related to analytical treatment of three-loop diagrams. Moreover, we have used them for independent crosschecks to verify obtained results. In the space dimension $d = 3$ ($\varepsilon = 1$), we have carried out the resummation technique using Padé approximants. Obtained results are in accordance with the prediction of critical exponents from a Monte Carlo simulations. We expect that in the next order of perturbation theory, the evaluation of critical exponents may provide even better results than simulations. In addition, in higher orders, it is possible to use other resummation methods built on Padé approximants with the Borel-Leroy transformation [66] or the Conformal mapping [10].

This study presents a step towards enhancing multiloop calculations in nonequilibrium physics. It could help to solve other more involved dynamical models. There are several other directions in which this work can be extended. One conceivable task would be an analysis of universal amplitude ratios. Another potential direction would be even more sophisticated four-loop calculation, which would be beneficial for asymptotic analysis.

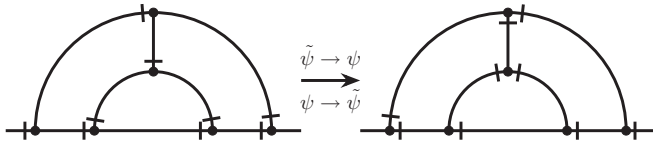


FIG. 2. Three-loop diagrams of DP process for two-point Green function $\Gamma^{(1,1)}$ bounded by rapidity-reversal symmetry (4).

ACKNOWLEDGMENTS

The work was supported by VEGA Grant No. 1/0535/21 of the Ministry of Education, Science, Research and Sport of the Slovak Republic and by the grant of the Slovak Research and Development Agency under the Contract No. APVV-21-0319.

APPENDIX: SYMMETRY PROPERTIES

In this Appendix, the relationships between self-energy and vertex diagrams will be obtained, which were used to verify the calculations.

The symmetry relations (4) with respect to time reversal can be used to find connections between diagrams, e.g., it is possible to find identical diagrams among self-energy diagrams and vertex diagrams. For self-energy diagrams, this follows directly from the fact that transformation (4) transforms the self-energy graphs $\langle \psi \tilde{\psi} \rangle_{1PI}$ into $\langle \tilde{\psi} \psi \rangle_{1PI}$. In Fig. 2, the example of such a transformation is demonstrated, explicitly showing the equality of the depicted diagrams.

In some cases, such a transformation does not provide information—it leads to identical equality, as, for example, for the one-loop diagram (53) and both two-loop diagrams (54). For three-loop self-energy functions, in addition to the relations determined in Fig. 2, there are also four nontrivial identities.

By means of relations (4) the vertex function $\Gamma^{(1,2)}$ is transformed to the $\Gamma^{(2,1)}$. Figure 3 shows how it is possible to replace the upper outer tail $\tilde{\psi}$ with ψ , which gives information about the equality of two different diagrams $\Gamma^{(1,2)}$. This procedure is not informative for every vertex diagram, for example, in Fig. 4 it is impossible to replace any of the outer tails $\tilde{\psi}$ with ψ in the second diagram, since this would give rise to a triple vertex $\Gamma^{(0,3)}$ that is, however, absent in theory. This situation takes place for all diagrams $\Gamma^{(1,2)}$ in which both outer tails are connected to two fields $\tilde{\psi}$, as in the example considered. As a result, for the 1PI diagrams of the Green function $\Gamma^{(1,2)}$, 52 equalities of identical pairs of diagrams were obtained.

Some additional connections between the values of three-loop diagrams can be obtained using the equality

$$\text{---} \text{---} \text{---} \text{---} \text{---} = \text{---} \text{---} \text{---} \text{---} \text{---} \tag{A1}$$



FIG. 3. Example of a diagram for Green function $\Gamma^{(1,2)}$, which after substitution can be represented as another existing diagram of $\Gamma^{(1,2)}$.

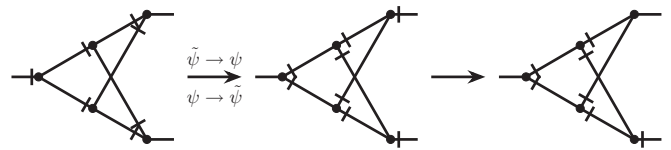


FIG. 4. Example of a diagram of $\Gamma^{(1,2)}$, which after the indicated substitution cannot be represented as a diagram of $\Gamma^{(1,2)}$ and has to be discarded from a consequent analysis.

One of its consequences is the equality of three pairs 1PI diagrams

$$\text{---} \text{---} \text{---} \text{---} \text{---} = \text{---} \text{---} \text{---} \text{---} \text{---} \tag{A2}$$

$$\text{---} \text{---} \text{---} \text{---} \text{---} = \text{---} \text{---} \text{---} \text{---} \text{---} \tag{A3}$$

$$\text{---} \text{---} \text{---} \text{---} \text{---} = \text{---} \text{---} \text{---} \text{---} \text{---} \tag{A4}$$

where the dotted external lines correspond to the use of equality (A1). Response fields should be added appropriately using the graphical rule for the interaction vertex (see Fig. 1).

A feature of the model (3) is the presence of a single propagator (16). This allows us to reconstruct all diagrams of 1PI functions (43) and (45) from the diagrams of function (46). Differentiating each propagator in the diagrams of the 1PI function (43) with respect to the external frequency, through which the frequency flows, and taking into account (16), gives

$$\partial_{i\omega} \left[\frac{1}{-i(\omega + \omega') + \varepsilon_k} \right] = \left[\frac{1}{-i(\omega + \omega') + \varepsilon_k} \right]^2 \tag{A5}$$

where ω' and k are the frequency and momentum of integration and ε_k was introduced in Eq. (16). In diagrammatic language, this relation can be written as

$$\partial_{i\omega} \text{---} \text{---} \text{---} = \text{---} \text{---} \text{---} = \text{---} \text{---} \text{---} \tag{A6}$$

The first equality is directly equivalent to relation (A5), the additional line in the second equality depicts the outer tail of the diagram, its insertion does not change the integrand for the diagram and turns it into the corresponding diagram for the three-point function. Note that when calculating function (43), the external frequency after differentiation $\partial_{i\omega}$ is assumed to be equal to zero, as well as when calculating function (46).

Thus, differentiation with respect to frequency when calculating the diagrams of function (43) can be replaced by

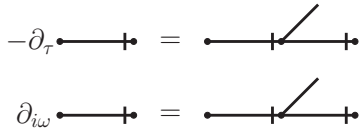


FIG. 5. Graphical representation of differentiation of DP propagator with respect to the τ (top), and with respect to the frequency ω (bottom).

the sum of diagrams of the form (46). Figure 5 displays an example of such a replacement for two different directions of external momentum leakage. Since the result does not depend on this direction, the right-hand sides of the equalities have to coincide, which can serve as a check of the correctness of the calculation of three-point diagrams.

Equalities (A5) and (A6) remain valid after the replacement $\partial_{i\omega} \rightarrow \partial_{\tau_0}/D_0$. Corresponding graphical rules are depicted in Fig. 6. This means that the sum of the contributions when differentiating each line when calculating the 1PI function (45) can be replaced by the sum of the corresponding three-tailed diagrams in function (46).

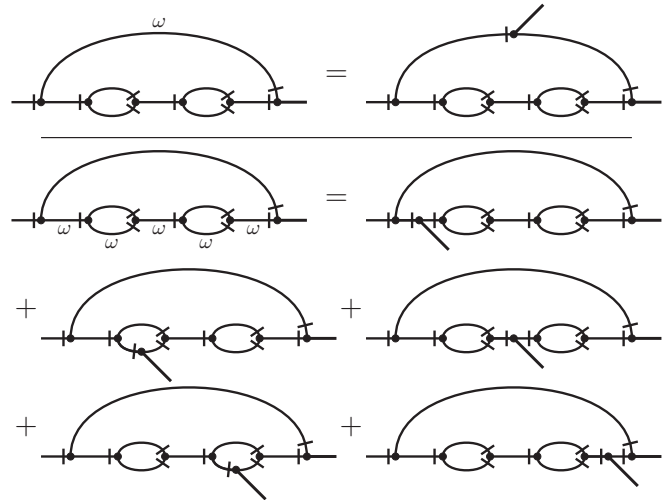


FIG. 6. Specific two-point diagram of DP process with two different possibilities for the flow of the external frequency ω . Propagators through which ω is flowing are subsequently replaced in all possible manner to yield a sum of corresponding three-point diagrams.

- [1] J. Marro and R. Dickman, *Nonequilibrium Phase Transitions in Lattice Models*, Collection Alea-Saclay: Monographs and Texts in Statistical Physics (Cambridge University Press, Cambridge, UK, 1999).
- [2] P. L. Krapivsky, S. Redner, and E. Ben-Naim, *A Kinetic View of Statistical Physics* (Cambridge University Press, Cambridge, UK, 2010).
- [3] P. A. Davidson, *Turbulence: An Introduction for Scientists and Engineers*, 2nd ed. (Oxford University Press, Oxford, 2015).
- [4] M. C. Cross and P. C. Hohenberg, *Rev. Mod. Phys.* **65**, 851 (1993).
- [5] J. B. Marston, *Annu. Rev. Condens. Matter Phys.* **3**, 285 (2012).
- [6] X. Fang, K. Kruse, T. Lu, and J. Wang, *Rev. Mod. Phys.* **91**, 045004 (2019).
- [7] P. C. Hohenberg and B. I. Halperin, *Rev. Mod. Phys.* **49**, 435 (1977).
- [8] U. C. Täuber, *Critical Dynamics: A Field Theory Approach to Equilibrium and Non-equilibrium Scaling Behavior* (Cambridge University Press, Cambridge, UK, 2014).
- [9] A. N. Vasil'ev, *The Field Theoretic Renormalization Group in Critical Behavior Theory and Stochastic Dynamics* (CRC Press, Boca Raton, FL, 2004).
- [10] J. Zinn-Justin, *Quantum Field Theory and Critical Phenomena* (Oxford University Press, Oxford, 2002).
- [11] J. Zinn-Justin, *Phase Transitions and Renormalization Group* (Oxford University Press, Oxford, 2007).
- [12] M. Kardar, *Statistical Physics of Fields* (Cambridge University Press, Cambridge, UK, 2007).
- [13] S. R. Broadbent and J. M. Hammersley, in *Mathematical Proceedings of the Cambridge Philosophical Society* (Cambridge University Press, Cambridge, UK, 1957), Vol. 53, pp. 629–641.
- [14] J. D. Murray, *Mathematical Biology: I. An Introduction*, 3rd ed. (Springer, Berlin, 2002).
- [15] H. Hinrichsen, *Adv. Phys.* **49**, 815 (2000).
- [16] M. Moshe, *Phys. Rep.* **37**, 255 (1978).
- [17] J. L. Cardy and R. L. Sugar, *J. Phys. A: Math. Gen.* **13**, L423 (1980).
- [18] U. C. Täuber, *J. Phys. A: Math. Theor.* **45**, 405002 (2012).
- [19] G. Ódor, *Rev. Mod. Phys.* **76**, 663 (2004).
- [20] T. M. Liggett, *Interacting Particle Systems* (Springer Science & Business Media, New York, 2012), Vol. 276.
- [21] E. V. Albano, *Physica A* **216**, 213 (1995).
- [22] Y. Pomeau, *Physica D* **23**, 3 (1986).
- [23] G. Lemoult, L. Shi, K. Avila, S. V. Jalikop, M. Avila, and B. Hof, *Nat. Phys.* **12**, 254 (2016).
- [24] M. Sano and K. Tamai, *Nat. Phys.* **12**, 249 (2016).
- [25] M. Sahimi, *Applications of Percolation Theory* (CRC Press, Boca Raton, FL, 2003).
- [26] H.-K. Janssen, *Z. Phys. B* **42**, 151 (1981).
- [27] P. Grassberger, *Z. Phys. B* **48**, 255 (1982).
- [28] S. Lübeck and R. D. Willmann, *Nucl. Phys. B* **718**, 341 (2005).
- [29] M. Henkel, H. Hinrichsen, and S. Lübeck, *Non-equilibrium Phase Transitions* (Springer, Berlin, 2008), Vol. 1.
- [30] K. A. Takeuchi, M. Kuroda, H. Chaté, and M. Sano, *Phys. Rev. Lett.* **99**, 234503 (2007).
- [31] K. A. Takeuchi, M. Kuroda, H. Chaté, and M. Sano, *Phys. Rev. E* **80**, 051116 (2009).
- [32] M. Sipos and N. Goldenfeld, *Phys. Rev. E* **84**, 035304(R) (2011).
- [33] P. M. Chaikin and T. C. Lubensky, *Principles of Condensed Matter Physics* (Cambridge University Press, Cambridge, UK, 1995).
- [34] D. J. Amit and V. Martín-Mayor, *Field Theory, the Renormalization Group, and Critical Phenomena: Graphs to Computers* (World Scientific, Singapore, 2005).
- [35] T. Vojta, *Phys. Rev. E* **86**, 051137 (2012).
- [36] I. Jensen, *J. Phys. A: Math. Gen.* **29**, 7013 (1996).

- [37] E. Carlon, M. Henkel, and U. Schollwöck, *Eur. Phys. J. B* **12**, 99 (1999).
- [38] L. Canet, B. Delamotte, O. Deloubrière, and N. Wschebor, *Phys. Rev. Lett.* **92**, 195703 (2004).
- [39] I. Jensen, *Phys. Rev. A* **45**, R563 (1992).
- [40] C. M. Bender and S. A. Orszag, *Advanced Mathematical Methods for Scientists and Engineers* (McGraw–Hill, New York, 1978).
- [41] H.-K. Janssen, *J. Stat. Phys.* **103**, 801 (2001).
- [42] H.-K. Janssen and U. C. Täuber, *Ann. Phys.* **315**, 147 (2005).
- [43] L. T. Adzhemyan, N. V. Antonov, M. V. Kompaniets, and A. N. Vasil'ev, *Int. J. Mod. Phys. B* **17**, 2137 (2003).
- [44] L. Ts. Adzhemyan, M. Hnatič, M. Kompaniets, T. Lučivjanský, and L. Mižišin, *EPJ Web Conf.* **108**, 02005 (2016).
- [45] L. Ts. Adzhemyan, M. Hnatič, M. Kompaniets, T. Lučivjanský, and L. Mižišin, *EPJ Web Conf.* **173**, 02001 (2018).
- [46] L. Ts. Adzhemyan, M. Hnatič, M. Kompaniets, T. Lučivjanský, and L. Mižišin, in *11th Chaotic Modeling and Simulation International Conference*, edited by C. H. Skiadas and I. Lubashevsky (Springer International Publishing, Cham, 2019), p. 195.
- [47] See Supplemental Material at <http://link.aps.org/supplemental/10.1103/PhysRevE.107.064138> for more technical details.
- [48] M. Doi, *J. Phys. A: Math. Gen.* **9**, 1465 (1976).
- [49] M. Doi, *J. Phys. A: Math. Gen.* **9**, 1479 (1976).
- [50] U. C. Täuber, M. Howard, and B. P. Vollmayr-Lee, *J. Phys. A: Math. Gen.* **38**, R79 (2005).
- [51] M. Hnatič, J. Honkonen, and T. Lučivjanský, *Acta Phys. Slovaca* **66**, 69 (2016).
- [52] C. W. Gardiner, *Handbook of Stochastic Methods* (Springer, Berlin, 2004).
- [53] H. K. Janssen, *Z. Phys. B* **23**, 377 (1976).
- [54] H. K. Janssen, *On the Renormalized Field Theory of Nonlinear Critical Relaxation: From Phase Transitions to Chaos*, edited by G. Györgyi, I. Kondor, L. Sasvári, and T. Tél (World Scientific, Singapore, 1992).
- [55] J. Honkonen, [arXiv:1102.1581](https://arxiv.org/abs/1102.1581).
- [56] C. de Dominicis, *J. Phys. Colloq. France* **37**, 1 (1976).
- [57] A. N. Vasil'ev, *Functional Methods in Quantum Field Theory and Statistical Physics* (Gordon & Breach Science, Amsterdam, 1998).
- [58] L. T. Adzhemyan, E. V. Ivanova, M. V. Kompaniets, and S. Y. Vorobyeva, *J. Phys. A: Math. Theor.* **51**, 155003 (2018).
- [59] T. Binoth and G. Heinrich, *Nucl. Phys. B* **585**, 741 (2000).
- [60] T. Hahn, *Comput. Phys. Commun.* **168**, 78 (2005).
- [61] J. F. Nagle, *J. Math. Phys.* **7**, 1588 (1966).
- [62] B. G. Nickel, D. I. Meiron, and J. G. A. Baker, University of Guelph report (1977).
- [63] D. Batkovich, Y. Kirienko, M. Kompaniets, and S. Novikov, [arXiv:1409.8227](https://arxiv.org/abs/1409.8227), program repository: https://bitbucket.org/mkompan/graph_state/downloads.
- [64] S. Lübeck, *Int. J. Mod. Phys. B* **18**, 3977 (2004).
- [65] L. T. Adzhemyan, N. V. Antonov, and A. N. Vasil'ev, *The Field Theoretic Renormalization Group in Fully Developed Turbulence* (Gordon & Breach, London, 1999).
- [66] L. T. Adzhemyan, E. V. Ivanova, M. V. Kompaniets, A. Kudlis, and A. I. Sokolov, *Nucl. Phys. B* **940**, 332 (2019).
- [67] M. Borinsky, J. A. Gracey, M. V. Kompaniets, and O. Schnetz, *Phys. Rev. D* **103**, 116024 (2021).
- [68] R. Dickman, *Phys. Rev. E* **60**, R2441 (1999).
- [69] J. Wang, Z. Zhou, Q. Liu, T. M. Garoni, and Y. Deng, *Phys. Rev. E* **88**, 042102 (2013).